CMS Physics Analysis Summary

Contact: cms-pag-conveners-b2g@cern.ch 2013/03/11

Search for narrow t + b resonances in the leptonic final state at $\sqrt{s}$ = 8 TeV

The CMS Collaboration

Abstract

We present a search for the production of a heavy gauge boson W′ decaying into a top quark and a bottom quark using a dataset collected during 2012 by the CMS experiment at $\sqrt{s} = 8$ TeV, corresponding to an integrated luminosity of 19.6 fb^{-1}. We study different models of W′ boson production in the W′ to tb decay mode, investigating an arbitrary combination of left- and right-handed couplings. The analysis is based on events with the final state signature lepton (e, μ) plus jets and missing transverse energy. We find no evidence for W′ boson production and set 95% C.L. upper limits on the production cross-section. For W′ bosons with purely right-handed couplings, and for those with left-handed couplings when ignoring interference with the Standard Model, the observed (expected) 95% C.L. limit is $M_{W'} > 2.03(2.09)$ TeV.

1 Introduction

Charged massive gauge bosons, usually called W', are predicted by various extensions of the Standard Model (SM) [1–5]. One of the most promising ways to search for a W' boson is through the decay to third generation quarks $W' \to tb$ ($t\bar{b} + \bar{t}b$). This channel is important because in many models the third generation is expected to be coupled more strongly to the W' than the first and second generations [6, 7]. In addition, it is easier to suppress continuum multijet background for the decay $W' \to tb$ than for a generic $W' \to qq'$ decay. In contrast to $W' \to \ell\nu$ decays, the tb final state is, up to a quadratic ambiguity, fully reconstructable, which means that W' resonant mass structures may be searched for, even in the case of wider W' resonances.

Searches in this channel have been performed at the Tevatron [8, 9] and at the LHC [10, 11]. The CMS search [10] at $\sqrt{s} = 7$ TeV set a limit of 1.85 TeV for W' bosons with purely right-handed couplings. If the W' has left-handed couplings, interference between $W' \to tb$ and SM single-top quark production via $W \to tb$ can contribute as much as 5–20% of the total W' rate, depending on the W' mass and its couplings [12]. The $\sqrt{s} = 7$ TeV search took this interference effect into account and put constraints on an arbitrary set of left- and right-handed couplings of the W' bosons.

This note describes an update of the analysis described in Ref. [10] using data collected by the CMS experiment [13] corresponsding to an integrated luminosity of 19.6 fb^{-1} at $\sqrt{s} = 8$ TeV. For a 2 TeV W' boson, the production cross-section is larger by a factor of approximately 2 at $\sqrt{s} = 8$ TeV compared to $\sqrt{s} = 7$ TeV. The integrated luminosity analyzed in this search is larger than the $\sqrt{s} = 7$ TeV dataset by a factor of approximately 4. As before, we analyze events with the final state signature of lepton (e, μ) plus jets and missing transverse energy (E_T^{miss}) from the decay chain $W' \to tb$, $t \to bW \to b\ell\nu$, for an arbitrary combination of left- and right-handed couplings.

2 Signal and Background Modeling

2.1 Signal Modeling

The most general, model independent, lowest order effective interaction Lagrangian of the W' boson to SM fermions can be written as

$$\mathcal{L} = \frac{V_{f_i f_j}}{2\sqrt{2}} g_w \overline{f}_i \gamma_\mu \left(a^R_{f_i f_j}(1+\gamma^5) + a^L_{f_i f_j}(1-\gamma^5)\right) W'^{\mu} f_j + \text{H.c.}\,, \tag{1}$$

where $a^R_{f_i f_j}, a^L_{f_i f_j}$ are the right- and left-handed couplings of the W' boson to fermions f_i and f_j, $g_w = e/(s_w)$ is the SM weak coupling constant and $V_{f_i f_j}$ is the CKM matrix element if the fermion (f) is a quark, and $V_{f_i f_j} = \delta_{ij}$ if it is a lepton, where δ_{ij} is the Kronecker delta and i, j are the generation numbers. The notations are defined such that for a so-called SM-like W' boson $a^L_{f_i f_j} = 1$ and $a^R_{f_i f_j} = 0$.

The signal modeling is identical to that in Ref. [10]. In order to simulate the general coupling dependence we study MC samples for different cases separately [12]: samples of W' bosons with purely left-handed couplings, samples of W' bosons with purely right-handed couplings, and samples of W' with mixed couplings. For all generated signal samples the following nomenclature is used:

- "SM+W'_L" i.e. $a^L_{ud} = a^L_{cs} = a^L_{tb} = 1$, $a^R_{ud} = a^R_{cs} = a^R_{tb} = 0$,
- "W'_R" i.e right-handed W' with $a^L_{ud} = a^L_{cs} = a^L_{tb} = 0$, $a^R_{ud} = a^R_{cs} = a^R_{tb} = 1$.
- "SM+W'_{mixed}" i.e. $a^L_{ud} = a^L_{cs} = a^L_{tb} = 1$, $a^R_{ud} = a^R_{cs} = a^R_{tb} = 1$,

The differences between W' bosons with left- and right-handed couplings that are relevant for our search are that W'_L bosons which have left-handed couplings couple to the same fermion multiplets as the Standard Model W boson and therefore there will be interference between the two tb production diagrams with a W boson and with a W'_L boson. W'_R bosons with purely right-handed couplings couple to different final state particles and therefore do not interfere with the Standard Model W boson. Since their leptonic decays involve a right-handed neutrino ν_R of unknown mass they may only be allowed to decay to qq' final states, if $M_{\nu_R} > M_{W'}$, or they may decay to $\ell\nu$ and qq' final states, if $M_{\nu_R} < M_{W'}$, leading to different branching fractions for $W' \to$ tb. In the absence of interference between W and W' and if $M_{\nu_R} < M_{W'}$, there is no difference between W'_L and W'_R for our search.

In order to extend the analysis to higher masses, W' bosons are simulated at mass values ranging from 0.8 to 3.0 TeV. The factorization scale is set to the W' boson mass for the generation of the COMPHEP samples and also to compute the leading order (LO) cross-section. This LO cross-section is then scaled to NLO using a k-factor of 1.2 based on Ref. [14, 15]. The uncertainty on the cross-section is about 8.5% and includes contributions from the NLO scale (3.3%), PDFs (7.6%), α_s (1.3%) and the top quark mass ($< 1\%$).

2.2 Background Modeling

The $W' \to$ tb decay is characterized by the presence of a high-p_T isolated lepton, significant E_T^{miss} associated with the undetected neutrino, and at least two high-p_T b-jets. The primary sources of background are $t\bar{t}$, W+jets, single top (tW, s-, and t-channel), Z/γ^*+jets, and diboson production (WW). Background contributions are estimated from Monte Carlo (MC) simulation and further correction factors derived from data are applied to ensure agreement with the data. Both the signal and background parton-level samples are processed with PYTHIA [16] for parton fragmentation and hadronization. The simulation of the CMS detector is performed using GEANT [17].

The W and Z+jets backgrounds are estimated using simulated events generated with MADGRAPH [18]. The $t\bar{t}$ samples are generated using the MADGRAPH generator and are normalized to the approximate Next-to-Next-to-Leading-Order (NNLO) cross-section [19]. The SM single top (tW, s- and t-channel) backgrounds are estimated using simulated samples generated with POWHEG [20], normalized to the approximate NNLO cross-section [19]. For the W'_R search, s-channel, t-channel and tW single top events are considered as backgrounds. In the analysis for W'_L and W'_{mixed} bosons, due to interference between s-channel single top production and W', only t-channel and tW contribute to the backgrounds. The diboson (WW) background is generated with PYTHIA.

For all simulated samples, the additional proton-proton interactions in each bunch crossing (pile-up) were modeled by superimposing generated minimum-bias interactions onto simulated events, weighted such that the interaction multiplicity agrees with the luminosity profile of the data set used.

3 Object and Event Selection

Candidate events are required to have at least one reconstructed primary vertex. Leptons, jets and $E_{\mathrm{T}}^{\mathrm{miss}}$ are reconstructed using the Particle Flow (PF) algorithm [21].

Exactly one lepton is required to be within the detector acceptance ($|\eta| < 2.5$ for electrons excluding the barrel-end cap transition region, and $|\eta| < 2.1$ for muons) and to have fired an isolated electron or muon trigger. Electrons and muons are required to satisfy $p_{\mathrm{T}} > 50\,\mathrm{GeV}$ and also fulfill strict identification criteria. Electron candidates are selected using shower-shape information, the quality of the track, the match between the track and electromagnetic cluster, the fraction of total cluster energy in the hadronic calorimeter, and the amount of activity in the surrounding regions of the tracker and calorimeters. Events are removed whenever the electron is determined to originate from a converted photon. The track associated with a muon candidate is required to have at least one pixel hit, at least one hit in the muon detector, and a good quality global fit with $\chi^2/\mathrm{ndof} < 10$. Additionally, the cosmic ray background is eliminated by requiring the transverse impact parameter of the muon with respect to the beam spot be less than 2 mm. Electrons (muons) are required to have a Particle Flow based relative isolation within a cone of radius 0.3 (0.4) less than 0.10 (0.12). Events containing a second lepton with looser identification and isolation requirements are also rejected. Leptons are required to be separated from jets by $\Delta R(\mathrm{jet}, \ell) = \sqrt{\Delta\eta^2 + \Delta\phi^2} > 0.3$. To estimate the shape and yield of the W$'$ signal and backgrounds, corrections are derived using a tag and probe method in Z+jets events, and applied to MC in order to account for the differences in the lepton trigger, identification, and isolation efficiencies between data and MC.

Jets are clustered using the anti-k_T algorithm with a cone size of $\Delta R = 0.5$ [22] and required to satisfy $p_{\mathrm{T}} > 30\,\mathrm{GeV}$ and $|\eta| < 2.4$. At least two jets are required in the event with the leading jet $p_{\mathrm{T}} > 120\,\mathrm{GeV}$ and second leading jet $p_{\mathrm{T}} > 40\,\mathrm{GeV}$. Given that there are two b quarks in the final state, at least one of the two leading jets is then required to be tagged as a b-jet. We use the CSV tagger [23] with the medium operating point (CSVM). A data-to-MC b-tagging efficiency scale factor and a light-jet mistag rate scale factor were determined from MC and the 2012 data and applied on a jet-by-jet basis to all b-jets, c-jets, and light jets in the MC. Scale factors are also applied to W+jets events in which a bottom, charm, or light quark are produced in association with the W, in order to bring these yields into agreement with data. The procedure is identical to Ref. [10]. Based on lepton + jets samples with various jet multiplicites, W+b and W+c corrections are derived [24]. To account for differences between the lepton + jets topology and the topology considered here, additional W+light and W+b/c corrections are derived and applied. These corrections are 3% smaller and 7% larger, respectively, than the corrections derived in [10].

Finally, the $E_{\mathrm{T}}^{\mathrm{miss}}$ is required to exceed 20 GeV to reduce the QCD multijet background in both the electron and muon channels.

The observed number of events and the expected background yield after applying the above selection criteria are listed in Table 1. These numbers show very good agreement between the data and the simulation.

4 Data Analysis

The distinguishing feature of a W$'$ signal is a narrow resonance structure in the tb invariant mass. However, we cannot directly measure the tb invariant mass. Instead we reconstruct the invariant mass from the combination of the charged lepton, the neutrino, the jet which

Table 1: Number of selected data, signal, and background events. For the background samples, the expectation is computed corresponding to an integrated luminosity of 19.6 fb^{-1}. The final column for each channel includes the following cuts: $p_T^{\text{top}} > 85\,\text{GeV}$, $p_T^{\text{jet1,jet2}} > 140\,\text{GeV}$, 130< M_{top} <210 GeV.

Process	Number of Events					
	Electrons			Muons		
	b-tagged jets		Additional cuts	b-tagged jets		Additional cuts
	= 1	≥ 1		= 1	≥ 1	
Data	63050	72696	20238	62955	72820	20639
Signal:						
s-channel	176	269	86	197	299	96
M(W$'_R$ =) 1700 GeV	90	117	84	77	99	70
M(W$'_R$ =) 1900 GeV	41	52	37	35	44	31
M(W$'_R$ =) 2100 GeV	19	24	17	16	20	14
Background:						
$t\bar{t}$	36169	44575	14663	36989	45703	14923
t-channel	2124	2484	823	2287	2662	866
tW-channel	2571	2934	959	2659	3033	979
$W(\rightarrow \ell\nu)$+jets	19707	20263	3687	19438	20108	3717
$Z/\gamma^*(\rightarrow \ell\ell)$+jets	1492	1575	271	1505	1578	293
WW	206	216	50	220	226	49
Total Background	62269	72047	20452	63098	73310	20826
MC / Data	0.988	0.991	1.011	1.002	1.007	1.009

gives the best top quark mass reconstruction, and the highest p_T jet in the event which is not associated with the top quark. The xy-components of the neutrino momentum are taken from the missing transverse energy. The z-component is calculated by constraining the invariant mass of the lepton-neutrino pair to the W boson mass (80.4 GeV). This constraint leads to a quadratic equation in p_z^ν. In the case of two real solutions, both solutions are used to reconstruct W boson candidates. In the case of complex solutions, the real part is assigned to p_z^ν and the p_T of the neutrino is re-computed, choosing the p_T solution which gives the invariant mass of the lepton-neutrino pair closest to 80.4 GeV, resulting in a single W candidate. Top quark candidates are then reconstructed using the W candidate(s) and all of the selected jets in the event. The top candidate with mass closest to 172.5 GeV is chosen as the best representation of the top quark (M(W, bestjet)). The W$'$ invariant mass (M(bestjet, jet2, W)) is obtained by combining the "best" top quark candidate with the highest p_T jet (jet2) remaining after the top quark reconstruction.

Figure 1 shows the reconstructed tb invariant mass distribution for the data and W$'$ signal samples generated at four different mass values (1.8, 2.0, 2.5, and 3.0 TeV). Also included in the plots are the main background contributions. The data and background distributions are shown for sub-samples with one or more b-tags, separately for the electron and muon channels. Three additional criteria are imposed for improving the signal-to-background discrimination: the p_T of the best top candidate (closest in mass to the top quark) > 85 GeV, the p_T of the vector sum of the two leading jets p_T(jet1,jet2) > 140 GeV, and the best top mass candidate with 130 GeV $< M(\text{W}, \text{bestjet}) < 210$ GeV.

Since the W+jets process is one of the major backgrounds to the W$'$ signal (see Table 1), a study is performed to verify that the W+jets shape is modeled realistically in the simulation. This study utilizes the fact that events with zero b-tagged jets in data that satisfy all other

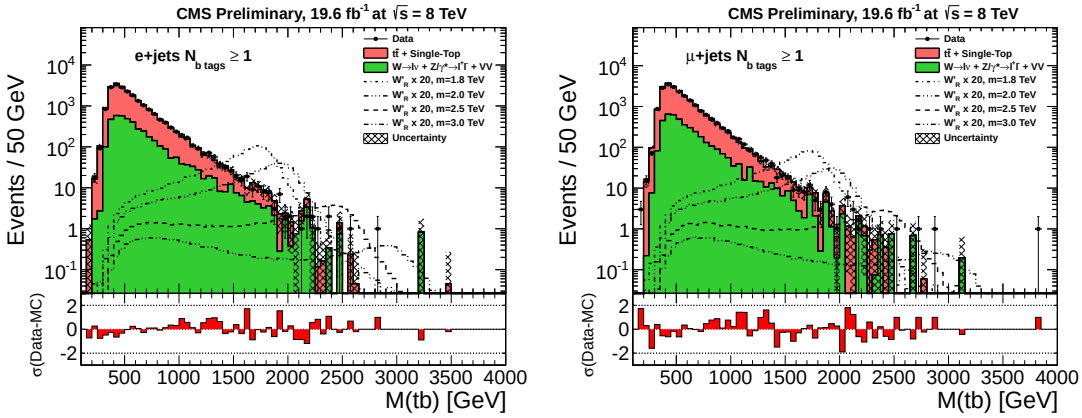

Figure 1: Reconstructed W$'$ invariant mass distributions after the full selection. Events with electrons (muons) are shown on the left panel (right panel) for data, background and four different W$'_R$ signal mass hypotheses (1.8, 2.0, 2.5, and 3.0 TeV). All events are required to have at least one b-tagged jet. The hatched bands represent the total uncertainty on the predicted backgrounds. For the purpose of illustration, the expectation for W$'$ signal samples are scaled by a factor of 20.

selection criteria are expected to originate predominantly from the W+jets background. These events are used to verify the shape of the W+jets background in data. The shape is obtained by subtracting the backgrounds other than W+jets from the data. The invariant mass distribution for events with zero b-tagged jets (derived from data) using this method shows agreement with the same distribution from the W+jets zero b-tagged Monte Carlo sample, thus validating the simulation. The difference between the distributions is included as a systematic uncertainty on the shape of the W+jets background. Using MC samples, it was also cross-checked that the W+jets background shape was independent of the number of b-tagged jets by comparing the mass distribution with zero b-tagged jets with one produced by requiring one or more b-tagged jets.

The top p_T distribution in data is not well modelled by the simulation. We therefore define a control region in data which is dominated by $t\bar{t}$ events in order to reweight the simulation to match the observed distribution. The cuts which define the control region are $N_{jets} \geq 4$,$N_{b-tags} \geq 2$, and $400 < M(tb) < 750$ GeV, which also ensure small potential signal contamination. We perform a fit to the ratio of data to expected background events using both a Landau and linear function and reweight the $t\bar{t}$ samples using the Landau fit. The linear fit and original distribution are used as systematic uncertainties on the $t\bar{t}$ shape.

5 Systematic Uncertainties

Systematic uncertainties were evaluated in two ways:

- Uncertainty on the normalization:
  This category includes uncertainties in the integrated luminosity (4.4%), object identification efficiencies (1%), and trigger modeling (1-2%). Also included are uncertainties related to obtaining the heavy flavor ratio from data [25].
- Uncertainties that change both the shape and normalization of the distributions:
  This category includes the uncertainty from the jet energy scale, the b-tagging and mis-tagging efficiency scale factors. For the W+jets samples, uncertainties on the light and heavy flavor scale factors are also included. The variation of the factoriza-

tion scale Q^2 used in the strong coupling constant $\alpha_s(Q^2)$, and the jet-parton matching scale [26] uncertainties are evaluated for the $t\bar{t}$ background sample. These uncertainties are evaluated by raising and lowering the corresponding correction by one standard deviation and repeating the whole analysis. For the W+jets, there is an additional systematic due to the shape difference between data and simulation as observed in the 0-b-tagged sample. For the $t\bar{t}$ sample, there is an additional systematic due to the reweighting of the top p_T spectrum from data.

6 Results

6.1 Cross-section limits

The observed $W^{'}$ mass distribution in the data and the prediction for the total expected background agree within uncertainties. We set upper limits on the $W^{'}$ boson production cross-section for different $W^{'}$ masses. The limits are computed using the Bayesian statistics approach of the theta package [27]. In order to reduce the statistical uncertainty, we bin the invariant mass distribution using 1 bin from 100 GeV to 300 GeV, 17 bins of 100 GeV width from 300 to 2000 GeV, and then two additional bins from 2000 to 2200 GeV and from 2200 to 4000 GeV. These are the input distributions to the limit setting procedure. A binned likelihood is used to calculate upper limits on the signal production cross-section times branching fraction: $\sigma(pp \rightarrow W^{'}) \times BR(W^{'} \rightarrow tb)$. The procedure accounts for the effects on normalization and shape due to systematic uncertainties as necessary (see Section 5), as well as limited statistics in the background templates. Expected cross-section limits for each $W^{'}{}_R$ boson mass are also computed as a measure of the sensitivity of the analysis. To obtain the best sensitivity, we also combine the muon and electron samples.

In the plots shown in Fig. 2 and 3, the black solid line denotes the observed limit and the red solid line represents the theoretical cross-section predictions. The lower mass limit is defined by the intersection of the line denoting the measured limit with the line for the nominal value of the theoretical cross-section.

These limits also apply to $W^{'}{}_L$ boson, if no interference with the SM is taken into account.

6.2 Limits on Coupling Strengths

The effective Lagrangian given by Eq. 1 can be analyzed for arbitrary combinations of left-handed a^L or right-handed a^R coupling strengths. The cross-section for single top quark production in the presence of a $W^{'}$ boson for any set of coupling values can be written in terms of the cross-sections σ_L for purely left-handed couplings $(a^L, a^R) = (1, 0)$, σ_R for purely right-handed couplings $(a^L, a^R) = (0, 1)$, σ_{LR} for mixed couplings $(a^L, a^R) = (1, 1)$, and σ_{SM} for SM couplings $(a^L, a^R) = (0, 0)$. It is given by:

$$\begin{aligned} \sigma &= \sigma_{SM} + a^L_{ud} a^L_{tb} \left(\sigma_L - \sigma_R - \sigma_{SM}\right) \\ &+ \left(\left(a^L_{ud} a^L_{tb}\right)^2 + \left(a^R_{ud} a^R_{tb}\right)^2 \right) \sigma_R \\ &+ \frac{1}{2} \left(\left(a^L_{ud} a^R_{tb}\right)^2 + \left(a^R_{ud} a^L_{tb}\right)^2 \right) \left(\sigma_{LR} - \sigma_L - \sigma_R\right). \end{aligned} \tag{2}$$

We assume that the couplings to first generation quarks, a_{ud}, which are important for the production of the $W^{'}$ boson, and the couplings to third generation quarks, a_{tb}, which are important for the decay of the $W^{'}$ boson, are equal. For given values of a^L and a^R, the distributions are obtained by combining the four samples according to Eq. (2).

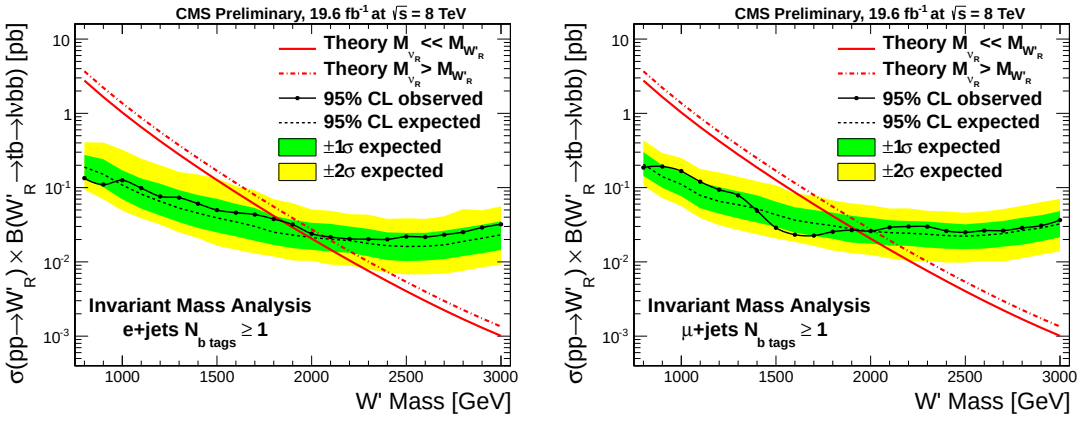

(a) (b)

Figure 2: The expected (dashed black line) and observed (solid black line) 95% C.L. upper limits on the production cross-section of right-handed $W^{'}$ bosons obtained for the electron (left) and muon (right) channels, along with the $\pm 1\sigma$ and $\pm 2\sigma$ uncertainty on the expected exclusion. The theoretical cross-section for right-handed $W^{'}$ production is shown as a solid (dot-dashed) red line, when assuming light (heavy) right-handed neutrinos.

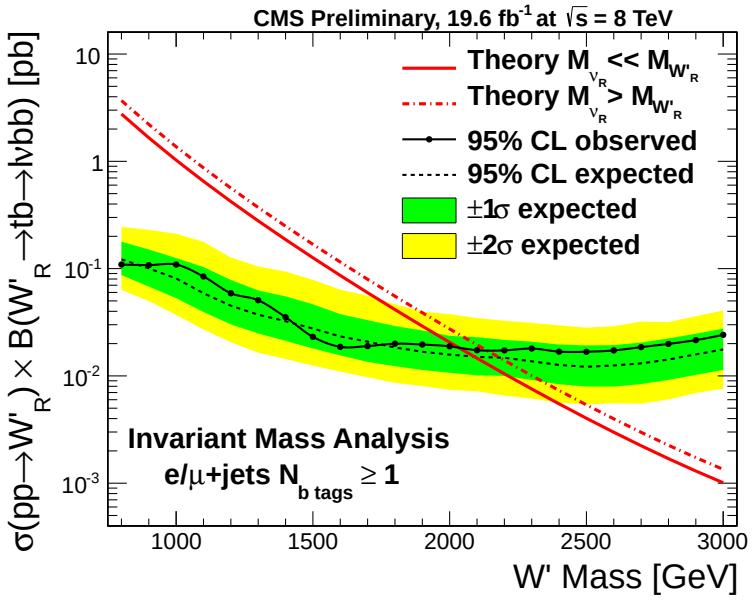

Figure 3: The expected (dashed black line) and observed (solid black line) 95% C.L. upper limits on the production cross-section of right-handed $W^{'}$ bosons obtained for the combination of the electron and muon channels, along with the $\pm 1\sigma$ and $\pm 2\sigma$ uncertainty on the expected exclusion. The theoretical cross-section for right-handed $W^{'}$ production is shown as a solid (dot-dashed) red line, when assuming light (heavy) right-handed neutrinos.

We vary both a^L and a^R between 0 and 1 in steps of 0.1, for each $W^{'}$ boson mass value. For each of these combinations of a^L, a^R, and $M(W^{'})$, we determine the expected and observed 95% C.L. upper limits on the cross-section. We can now assume values for a^L and a^R, and interpolate the cross-section limit in the mass value. The values of the $W^{'}$ mass for which the cross-section limit exceeds the theory cross-section are disfavored. Figure 4 shows the contours for the $W^{'}$ boson

mass in the (a^L, a^R) plane for which the cross-section limit equals the predicted cross-section. The contours are obtained using the W$'$ invariant mass distribution.

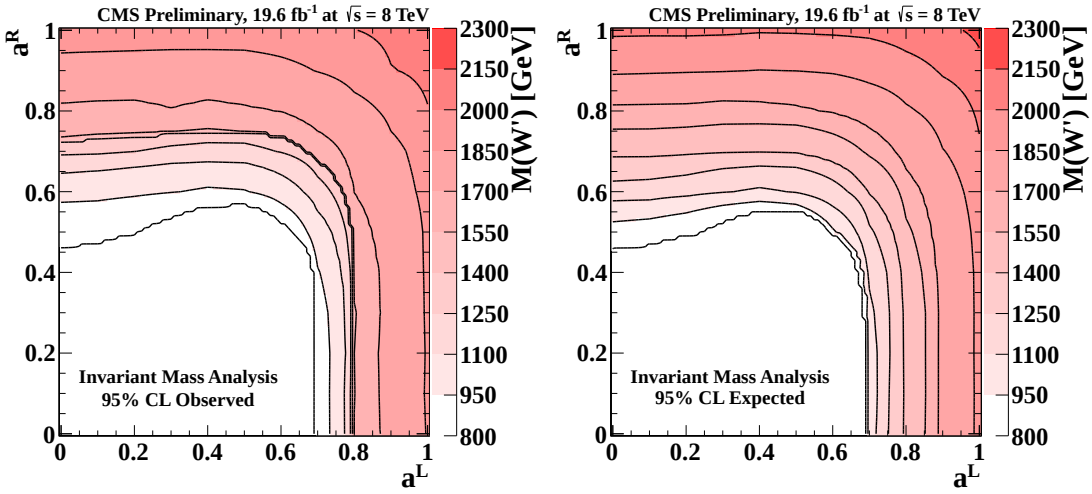

Figure 4: Contour plots of $M(\mathrm{W}')$ in the (a^L, a^R) plane at which the 95% C.L. cross-section limit equals the predicted cross-section for the combined e, μ+jets sample. The left (right) panel is for observed (expected) limits. The color axis is $M(\mathrm{W}')$ in GeV, and the solid black lines denote 150 GeV intervals of the W$'$ mass, starting from 800 GeV.

7 Conclusion

We have performed a search for W$'$ boson production in the tb decay channel using 19.6 fb^{-1} of data taken by the CMS detector. We find no evidence for W$'$ boson production and set 95% C.L. upper limits on the production cross-section for three different models of W$'$ production. We compare our measurement to the theoretical prediction for the nominal value of the cross-section to determine the lower limits on the mass of the W$'$. For W$'$ bosons with right-handed couplings to fermions (and for left-handed couplings to fermions, when no interference with SM is included) the observed (expected) limit is 2.03 TeV (2.09 TeV) at 95% C.L. These results represent an improvement over previously published results.

References

[1] M. Schmaltz and D. Tucker-Smith, "LITTLE HIGGS THEORIES", *Annual Review of Nuclear and Particle Science* **55** (2005), no. 1, 229–270, doi:10.1146/annurev.nucl.55.090704.151502.

[2] T. Appelquist, H.-C. Cheng, and B. A. Dobrescu, "Bounds on universal extra dimensions", *Phys. Rev. D* **64** (Jun, 2001) 035002, doi:10.1103/PhysRevD.64.035002.

[3] H.-C. Cheng et al., "Standard model in the latticized bulk", *Phys. Rev. D* **64** (Aug, 2001) 065007, doi:10.1103/PhysRevD.64.065007.

[4] R. S. Chivukula, E. H. Simmons, and J. Terning, "Limits on noncommuting extended technicolor", *Phys. Rev. D* **53** (May, 1996) 5258–5267, doi:10.1103/PhysRevD.53.5258.

[5] R. N. Mohapatra and J. C. Pati, "Left-right gauge symmetry and an 'isoconjugate' model of CP violation", *Phys. Rev. D* **11** (Feb, 1975) 566–571, doi:10.1103/PhysRevD.11.566.

[6] D. J. Muller and S. Nandi, "Topflavor: a separate SU(2) for the third family", *Physics Letters B* **383** (1996), no. 3, 345 – 350, doi:10.1016/0370-2693(96)00745-9.

[7] E. Malkawi, T. Tait, and C.-P. Yuan, "A model of strong flavor dynamics for the top quark", *Physics Letters B* **385** (1996), no. 14, 304 – 310, doi:10.1016/0370-2693(96)00859-3.

[8] The D0 Collaboration Collaboration, "Search for W' Boson Resonances Decaying to a Top Quark and a Bottom Quark", *Phys. Rev. Lett.* **100** (May, 2008) 211803, doi:10.1103/PhysRevLett.100.211803. http://link.aps.org/doi/10.1103/PhysRevLett.100.211803.

[9] D0, "Search for W$'$ resonances with left- and right-handed couplings to fermions", *Physics Letters B* **699** (2011), no. 3, 145 – 150, doi:10.1016/j.physletb.2011.03.066. http://www.sciencedirect.com/science/article/pii/S0370269311003510.

[10] CMS Collaboration, "Search for a W' boson decaying to a bottom quark and a top quark in pp collisions at $\sqrt{s} = 7$ TeV", arXiv:1208.0956.

[11] ATLAS Collaboration Collaboration, "Search for tb resonances in proton-proton collisions at $\sqrt{s} = 7$ TeV with the ATLAS detector", *Phys.Rev.Lett.* **109** (2012) 081801, doi:10.1103/PhysRevLett.109.081801, arXiv:1205.1016.

[12] E. Boos et al., "Interference between and W in single-top quark production processes", *Physics Letters B* **655** (2007), no. 5-6, 245 – 250, doi:10.1016/j.physletb.2007.03.064. http://www.sciencedirect.com/science/article/pii/S0370269307004157.

[13] CMS Collaboration, "The CMS experiment at the CERN LHC. The Compact Muon Solenoid experiment", *J. Instrum.* **3** (2008) S08004. 361 p. Also published by CERN Geneva in 2010.

[14] Z. Sullivan, "Fully differential W' production and decay at next-to-leading order in QCD", *Phys.Rev.* **D66** (2002) 075011, doi:10.1103/PhysRevD.66.075011, arXiv:hep-ph/0207290.

[15] D. Duffty and Z. Sullivan, "Model independent reach for W-prime bosons at the LHC", *Phys.Rev.* **D86** (2012) 075018, doi:10.1103/PhysRevD.86.075018, arXiv:1208.4858.

[16] T. Sjostrand, S. Mrenna, and P. Z. Skands, "PYTHIA 6.4 Physics and Manual", *JHEP* **0605** (2006) 026, doi:10.1088/1126-6708/2006/05/026, arXiv:hep-ph/0603175.

[17] S. J. Allison et al. *IEEE Trans. Nucl. Sci.* **53** (2006) 270.

[18] J. Alwall et al., "MadGraph/MadEvent v4: The New Web Generation", *JHEP* **09** (2007) 028, doi:10.1088/1126-6708/2007/09/028.

[19] N. Kidonakis, "NNLL threshold resummation for top-pair and single-top production", arXiv:1210.7813.

[20] S. Frixione, P. Nason, and C. Oleari, "Matching NLO QCD computations with Parton Shower simulations: the POWHEG method", *JHEP* **11** (2007) 070, doi:10.1088/1126-6708/2007/11/070.

[21] CMS Collaboration, "Commissioning of the particle-flow event reconstruction wi th leptons from J/ψ and W decays at 7 TeV", technical report, (2010).

[22] M. Cacciari, G. P. Salam, and G. Soyez, "The Anti-k(t) jet clustering algorithm", *JHEP* **0804** (2008) 063, doi:10.1088/1126-6708/2008/04/063, arXiv:0802.1189.

[23] CMS Collaboration, "Algorithms for b Jet identification in CMS",.

[24] CMS Collaboration Collaboration, "Measurement of the $t\bar{t}$ production cross section in pp collisions at 7 TeV in lepton + jets events using b-quark jet identification", *Phys. Rev. D* **84** (Nov, 2011) 092004, doi:10.1103/PhysRevD.84.092004.

[25] CMS Collaboration, "Performance of b-jet identification in CMS", *CMS Physics Analysis Summary* **CMS-PAS-BTV-12-001** (2012).

[26] J. Alwall et al., "Comparative study of various algorithms for the merging of parton showers and matrix elements in hadronic collisions", *Eur.Phys.J.* **C53** (2008) 473–500, doi:10.1140/epjc/s10052-007-0490-5, arXiv:0706.2569.

[27] T. Müller, J. Ott, and J. Wagner-Kuhr, "theta - a framework for template-based modeling and infere nce",. http://www-ekp.physik.uni-karlsruhe.de/~ott/theta/testing/ht\ml/theta__auto__intro.html.